

In this paper, a single switch three-phase ac to dc converter with reduced voltage stress is proposed. In the proposed converter, a coupled inductor and buffering capacitors are integrated to reduce the voltage stress on the main switch and diodes. The secondary winding of the coupled inductor is series-connected with a voltage buffering capacitor to reduce the voltage stress on the active switch. The switching loss of the proposed converter can be greatly reduced because of the lower voltage stress. As a result, the THD is effectively reduced and the converter efficiency is extremely increased about 10% higher than the conventional single switch DCM boost rectifier.

2 Three-phase ac to dc converters for micro-scale wind turbines

Fig. 1 shows the basic configuration of a micro-scale standalone wind power generation system. It is known that the wind power is a kind of unstable renewable power sources because the wind speed is always changing. Therefore an energy storage composed of a dc converter

and batteries is always required in the standalone system for buffering the wind power variation and stabilising the dc output power. For providing the output dc power, a three-phase ac to dc converter is required for extracting the wind power from the generator. The extracted wind power is maximised or limited by the three-phase ac to dc converter according to the load demand and the storage condition. The PMSG for small scale wind turbine can be equalised to a three-phase sinusoidal voltage source with three-phase inductances as shown in Fig. 2 [16, 17]. The three-phase inductances stand for the total inductances with consideration of the mutual inductances in the stator windings. In the three-phase model of PMSG, the equivalent series resistance of each phase is relatively small and could be negligible in small machines. Owing to the consideration of controller complexity, only the topologies with single switch are concerned in this study. A conventional topology of the three-phase ac to dc converters as shown in Fig. 2a is widely used because of the advantages of low cost and easy implementation. It is seen that the three-phase ac wind power is firstly converted into the pulsating dc power by a full-bridge diode rectifier. For micro-scale wind turbines, the diode rectifier is always followed by a boost dc converter for stepping up the voltage for dc link. There is only one active switch required to be controlled for extracting the wind power. However, the generator currents THD would be high because of the well-known disadvantage of the non-linearity of the full-bridge diode rectifier. The current THD would not only result in additional power losses but also the torque ripple to the shaft of the wind turbine. Moreover, the voltage stress of the active switch and diode in the boost dc converter are all equal to the dc bus voltage.

For improving the current THD, a single switch three-phase converter with DCM PFC shown in Fig. 2b is

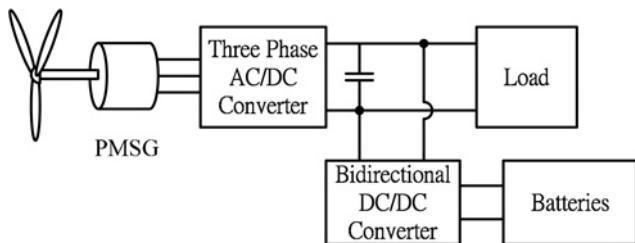


Fig. 1 Micro-scale standalone wind power generation system

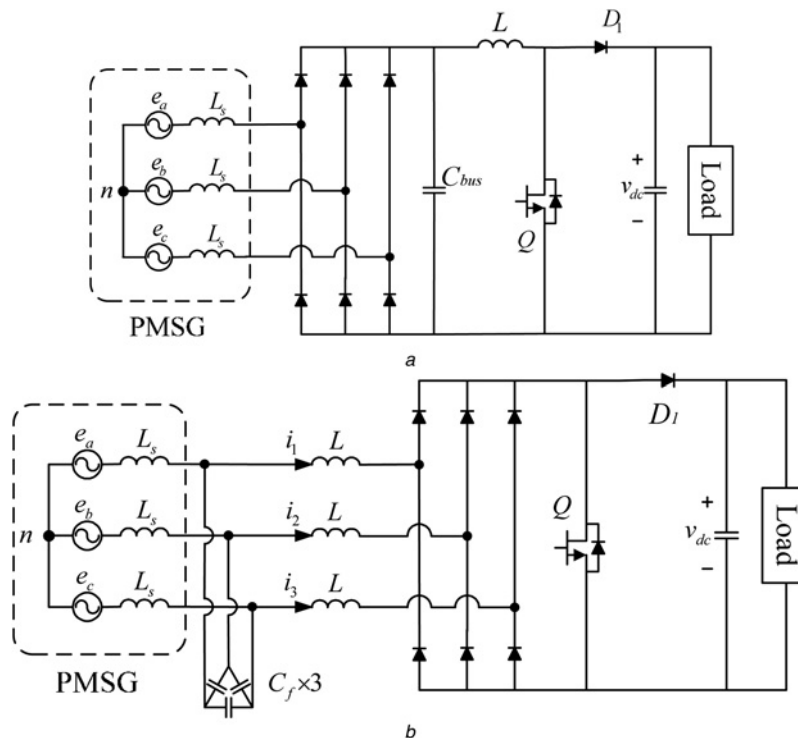


Fig. 2 Conventional single switch three-phase ac/dc converters

- a Two stages converter with diode bridge rectifier and boost dc converter
- b Single switch DCM PFC boost converter

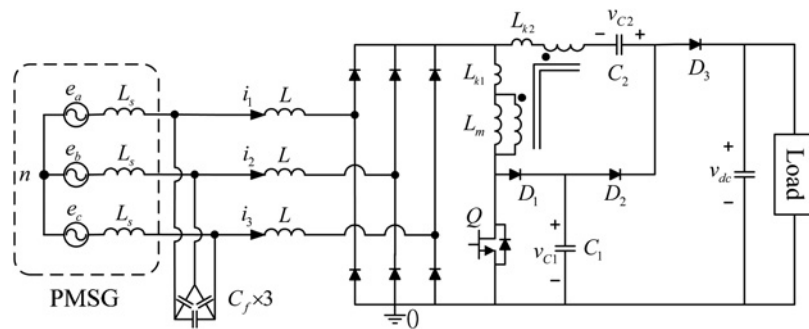


Fig. 3 Proposed single switch three-phase ac/dc converter

proposed in [6]. However, the voltage stresses of the active switch and the diodes are still equal to the dc bus voltage. Moreover, because of the high peak current from the DCM operation, the switch losses would be significant in this topology. To improve the mentioned disadvantages in the topology shown in Fig. 2b and keep the advantages of low-current THD and simple control topology, a coupled inductor and two buffering capacitors are integrated in the proposed converter as shown in Fig. 3 to reduce the voltage stresses. The DCM PFC technique is also adopted in the proposed converter to reduce current THD.

3 Operation principles of the proposed converter

According to relation between each phase voltage of the PMSG, there are six intervals in one cycle. The interval of $e_a > 0 > e_b > e_c$ is taken as an example for describing the operation principles of the proposed converter. It can be seen that the operation principles in the other intervals would be similar because of the symmetry of a balanced three-phase system. Basically, there are five operation modes in one switching cycle of the proposed converter

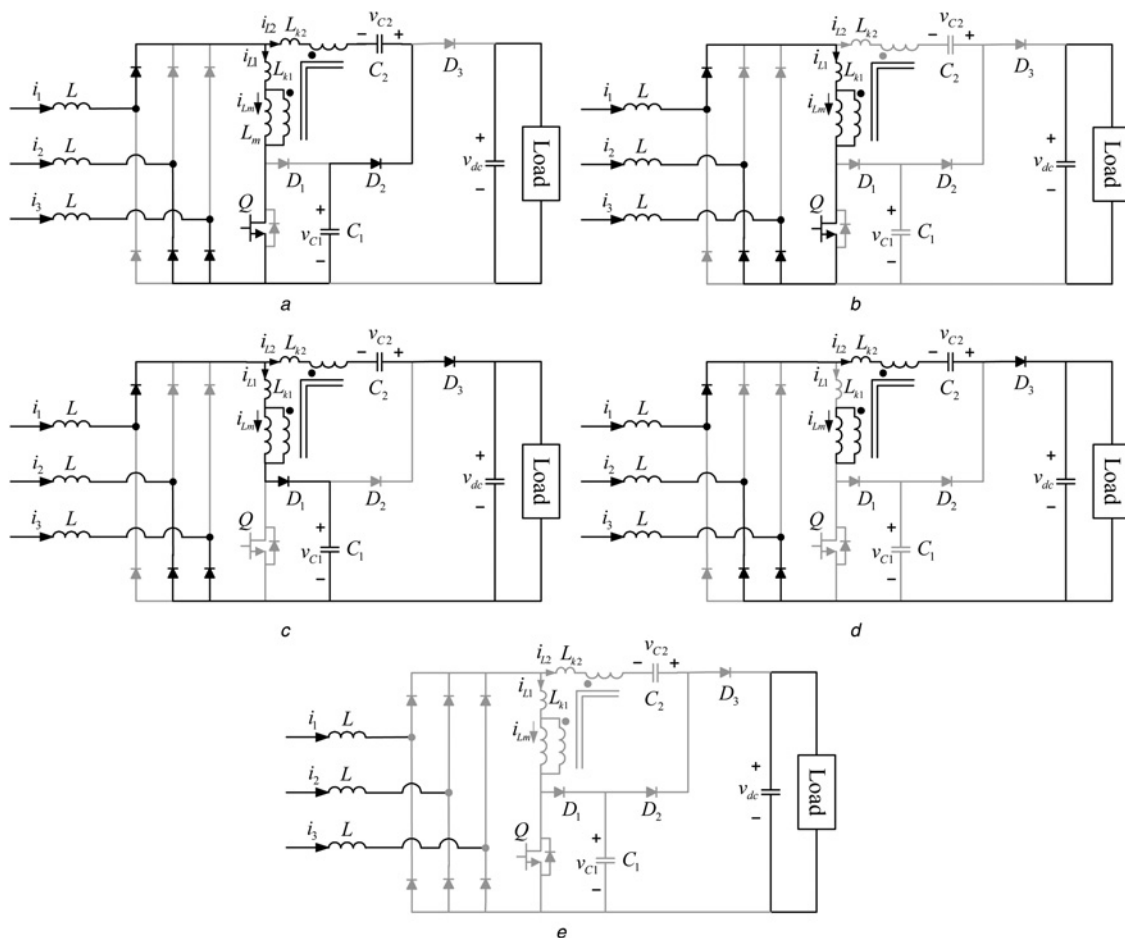


Fig. 4 Operation modes of the proposed converter

- a Mode I
- b Mode II
- c Mode III
- d Mode IV
- e Mode V

operated in this interval. Corresponding equivalent circuits in each operation mode are shown in Fig. 4. The output side is assumed to be connected to a well-regulated dc link. The dc-link voltage is always regulated by the energy storage composed of batteries and dc converters. The equivalent model of the coupled inductor is composed of primary leakage inductance L_{k1} , magnetising inductance L_m , secondary leakage inductance L_{k2} and an ideal transformer. The inductance of the coupled inductor is designed to be relatively much smaller than the input inductors. Therefore the voltage drop on the coupled inductor would be negligible. In the following analysis, all the components are assumed ideal. The relative waveforms of the active switch, diodes and coupled inductor are shown in Fig. 5.

(1) *Mode I* [t_0-t_1]: Owing to the DCM operation, the energy stored in the three input inductors L_1-L_3 should be totally released before $t=t_0$, that is, before starting this mode. Then, the active switch Q is turned on at $t=t_0$ for the wind power PM generator to deliver energy into the three input inductors L_1-L_3 . Each of the inductor currents is increased from zero with the slope approximately proportional to the corresponding input phase voltage. Because of the relation of the three phase back EMF in the interval, that is, $e_a > 0 > e_b > e_c$, the diodes D_{b1} , D_{b5} and D_{b6} are therefore turned on. Moreover, the secondary winding current i_{L2} would be reversely increased for the buffering capacitor C_2 to release

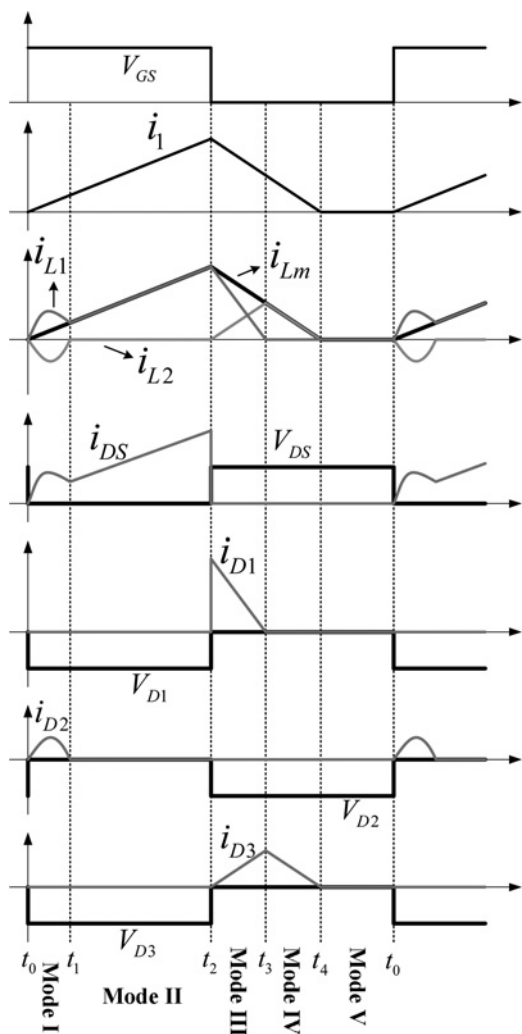


Fig. 5 Relative waveforms of the proposed converter

the pre-charged energy in the last mode to the buffering capacitor C_1 . Therefore the diode D_2 is conducting for this current loop. The energy stored in the coupled inductor is also increased in this mode. The primary winding current i_{L1} is then equal to the summation of the inductor current i_1 and the secondary current i_{L2} . While the discharging of capacitor C_1 is finished, the secondary current i_{L2} would become zero and the diode D_2 would be negatively biased for ending this mode. In this mode, the voltage stress of the diode D_3 is equal to $V_{dc} - V_{C1}$ and diode D_1 is reversely biased by the capacitor C_1 .

(2) *Mode II* [t_1-t_2]: In this mode, the active switch Q is still turned on and the diode D_2 is turned off. The primary current of the coupled inductor is equal to the inductor current i_1 because the loop of the secondary winding is opened, that is, $i_{L2} = 0$. It can be seen that the three input inductors L , the primary leakage L_{k1} and the magnetising inductance L_m are included in the conduction loop. Compared with the traditional three-phase DCM boost converter, the coupled inductor is added in the conduction loop. Therefore to keep the increasing slope of the current i_1 approximately proportional to the phase voltage e_a , the inductance of the coupled inductor should be sufficiently smaller than the input inductor for keeping the voltage drop on the coupled inductor negligible.

(3) *Mode III* [t_2-t_3]: At $t=t_2$, the active switch Q is turned off for releasing the energy stored in three input inductors L_1-L_3 to the load side. The diode D_1 is turned on to release the energy of the leakage inductance L_1 to the buffering capacitor C_1 . Therefore the voltage stress on the switch Q is clamped to the capacitor voltage V_{C1} . The voltage on the primary winding would then become negative because of the capacitor voltage V_{C1} and the induced voltage on the secondary winding would become negative as well. As a result, the diode D_3 is then forward biased and the secondary winding current i_{L2} starts to increase for transferring the energy on the magnetising inductance to the load side. The reverse voltage on the diode D_2 is therefore equal to $V_{dc} - V_{C1}$ because the diode D_3 is turned on in this mode. After the energy of the leakage inductance is totally released, that is, $i_{L1} = 0$, the diode D_1 is then turned off and this mode is ended at $t=t_3$.

(4) *Mode IV* [t_3-t_4]: In this mode, the diode D_3 is still turned on for continuously releasing the rest energy on the three input inductors and the magnetising inductance to the load side. It is seen that the secondary current i_{L2} is then equal to the input inductor current i_1 in this mode. Although all the energy stored in the three input inductors is totally released to the load side, that is, all the inductor currents are zero, the diode D_3 is then turned off and this mode is ended at $t=t_4$.

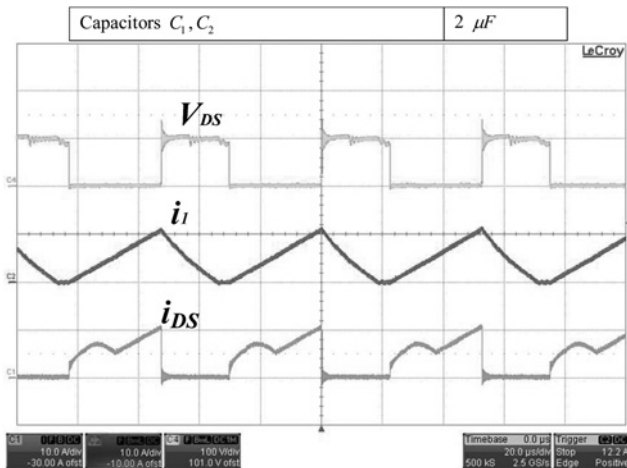
(5) *Mode V* [t_4-t_5]: In the last mode, the active switch and diodes all remained turned off. Therefore the output power is only provided by the output capacitor C in this mode. This mode is ended at $t=t_0$ and then the active switch Q would be turned on again for the next cycle of the five operation modes.

4 Experimental results

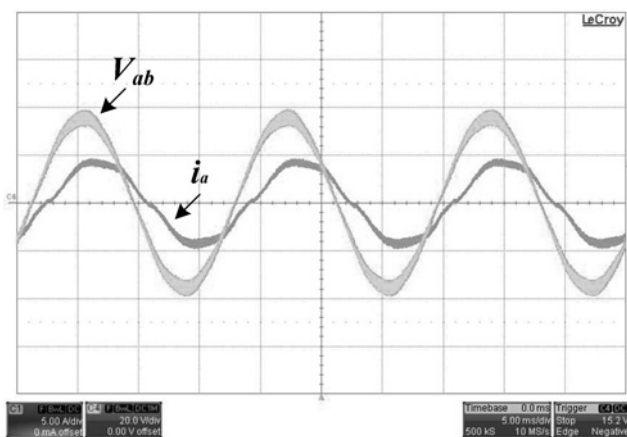
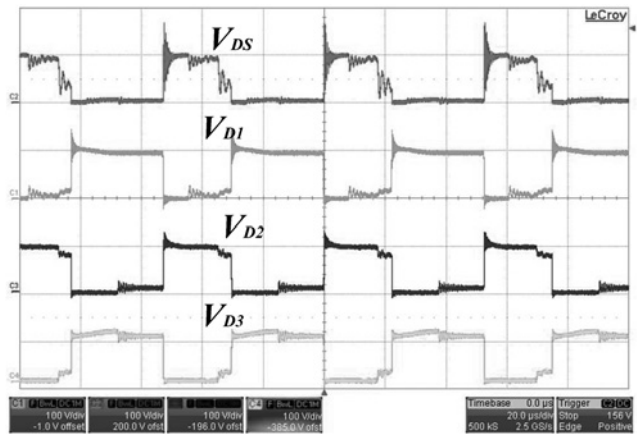
To evaluate the validity and the performance of the proposed converter, the prototype circuits of the traditional DCM boost PFC converter [6] and the proposed converter are both constructed with rated output power 200 W. The prototype circuit parameters are shown in Table 1. It can be seen that

Table 1 Prototype circuit parameters

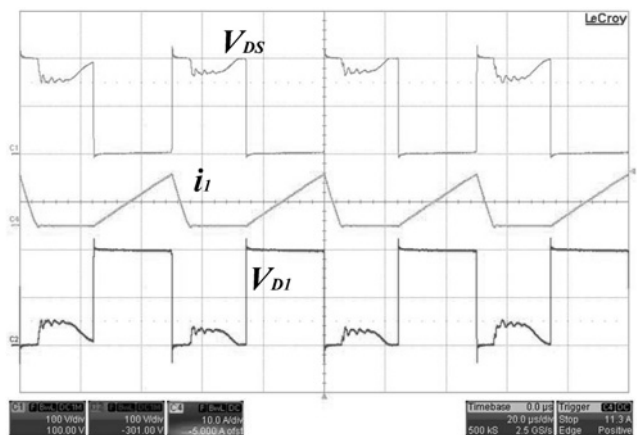
Rated power P_{rated}	200 W
DC bus voltage V_{DC}	200 V
Generator inductance L_s	100 μH
Generator equivalent series resistance R_s	40 m Ω
Filter capacitor C_f	4.7 μF
Boost inductor L	56 μH
Switching frequency f_s	20 kHz
Turn ratio of coupled inductor	1:1
Leakage inductances L_{k1}, L_{k2}	2 μH , 2 μH
Capacitors C_1, C_2	2 μF

**Fig. 6** Measured active switch voltage v_{DS} , input inductor current i_1 and active switch current i_{DS} (100 V/div; 10 A/div)

the generator equivalent series resistance of each phase is only 40 m Ω . The resistance could be reasonably neglected because the voltage drop on the resistance would be much smaller than the generator EMF. For example, if the generator phase current is 10 A, the voltage drop on the resistance would only be 0.4 V. Fig. 6 shows the waveforms of the active switch voltage v_{DS} , the input inductor current i_1 and the active switch current i_{DS} . The input inductor current i_1 is controlled at DCM for achieving power factor correction. The active switch current i_{DS} is composed of the input inductor current i_1 and the discharging current of capacitor

**Fig. 7** Measured terminal voltage and phase current of the wind generator (20 V/div; 5 A/div)**Fig. 8** Measured voltage waveforms on active switch Q and diodes D_1, D_2 and D_3 (100 V/div)

C_1 as illustrated in the operation mode I. The pulsating component in the input inductor current i_1 would be filtered out by the filter capacitor C_f . Fig. 7 shows the terminal voltage and phase current of the wind generator. It can be seen that the pulsating current on the input inductor current i_1 is filtered out and the phase current i_a is then nearly sinusoidal. The voltage waveforms of the active switch Q and the three diodes D_1, D_2 and D_3 are shown in Fig. 8. It is seen that all the voltage stresses are all reduced to half of the output dc voltage, that is, $\cong 100$ V. Fig. 9 shows the waveforms of active switch voltage v_{DS} , input inductor current i_1 and output diode voltage v_{D1} of the traditional DCM boost converter proposed in [6]. It is seen that the voltage stress of the main switch and diode is as high as the output voltage, that is, $\cong 200$ V. Fig. 10 shows the measured current THD and efficiency of the proposed converter and the DCM boost PFC converter within output power range 20–200 W. Compared with the traditional DCM boost PFC converter, the proposed single switch topology can efficiently reduce the current THD by about 2–6% for a micro-scale wind power generation system. The efficiency of the traditional converter is only about 80% because of the higher voltage stress and high-peak current because of DCM operation. The efficiency of the proposed converter is improved to about 91–92% because of reduced voltage stress and switching losses. Fig. 11 shows the input

**Fig. 9** Measured active switch voltage v_{DS} , input inductor current i_1 and output diode voltage v_{D1} of the traditional DCM boost converter (100 V/div; 10 A/div)

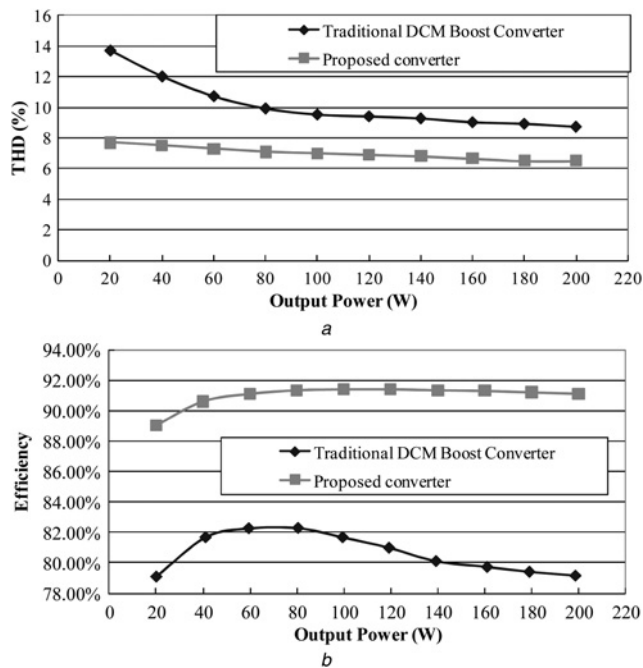


Fig. 10 Comparison between traditional DCM boost converter and proposed converter on

a Input current THD
b Efficiency

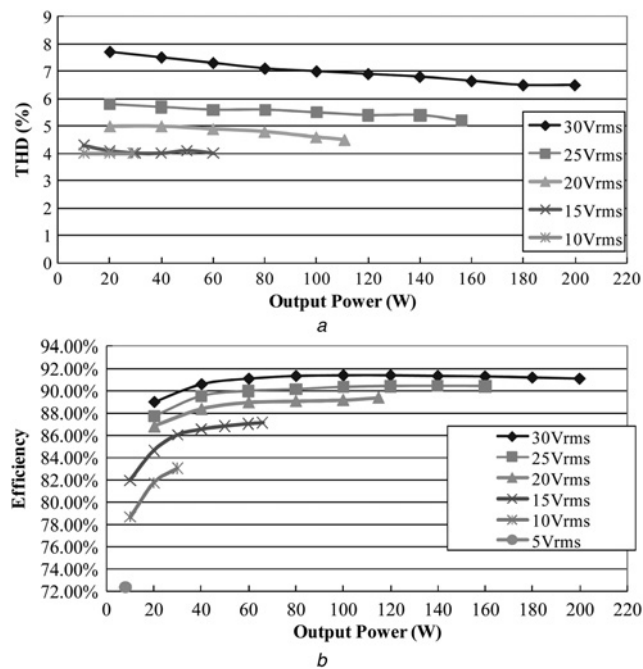


Fig. 11 Input current THD and efficiency of the proposed converter under different input voltage

current THD and efficiency of the proposed converter under different input voltage. It is well known that the maximum output power is theoretically proportional to the cube of the rotating speed of the permanent magnetic wind power generator and the terminal voltage is approximately proportional to the rotating speed. Therefore from Fig. 11, it can be seen that the proposed converter is capable of converting the ac power from the micro-scale wind power generator into a specific dc output power.

5 Conclusion

A single switch three-phase ac to dc converter with reduced voltage stress and current THD is proposed in this paper. A coupled inductor and two buffering capacitors are integrated to reduce the voltage stresses of the active switch and the diodes. As a result, the switching loss on the main switch can therefore be reduced. Both the prototype circuits of the traditional single switch DCM boost converter and the proposed converter are constructed for evaluation the performance. From the experimental results, it can be seen that the proposed converter can provide better performance on the wind generator current THD and the power conversion efficiency. The power conversion efficiency is greatly improved to about 92% which is 10% higher than the conventional single switch DCM boost converter and the current THD is reduced by about 2–6% as well. Moreover, the voltage stress on the main switch and diodes is greatly reduced to about half of the output dc voltage.

6 Acknowledgments

This work was supported in part by the National Science Council of R.O.C. under Grant NSC 101-2221-E-018-024 and Grant NSC 102-2221-E-018-011.

7 References

- 1 AWEA. (2010) 'AWEA Small Wind Turbine Global Market Study 2009', in the American Wind Energy Association Small Wind Systems. Available at: <http://www.awea.org/smallwind/>
- 2 AWEA. (2012 June) 'AWEA US Small Wind Turbine Market Report Year Ending 2011', in the American Wind Energy Association Small Wind Systems. Available at: <http://www.awea.org/smallwind/>
- 3 Koutroulis, E., Kalaitzakis, K.: 'Design of a maximum power tracking system for wind-energy-conversion applications', *IEEE Trans. Ind. Electron.*, 2006, **53**, (2), pp. 486–494
- 4 Knight, A.M., Peters, G.E.: 'Simple wind energy controller for an expanded operation range', *IEEE Trans. Energy Convers.*, 2005, **2**, (2), pp. 459–466
- 5 Malinowski, M., Stynski, S., Kolomyjski, W., Kazmierkowski, M.P.: 'Control of three-level PWM converter applied to variable-speed-type turbines', *IEEE Trans. Ind. Electron.*, 2009, **56**, (1), pp. 69–77
- 6 Prasad, A.R., Ziogas, P.D., Manias, S.: 'An active power factor correction technique for three-phase diode rectifiers', *IEEE Trans. Power. Electron.*, 1991, **6**, (1), pp. 83–92
- 7 Liserre, M., Blaabjerg, F., Hansen, S.: 'Design and control of an LCL-filter-based three-phase active rectifier', *IEEE Trans. Ind. Appl.*, 2005, **41**, (5), pp. 1281–1291
- 8 Yao, K., Ruan, X., Zou, C., Ye, Z.: 'Three-phase single-switch boost power factor correction converter with high input power factor', *IET Power. Electron.*, 2012, **5**, (7), pp. 1095–1103
- 9 Juan, Y.U.: 'An integrated-controlled AC/DC interface for microscale wind power generation systems', *IEEE Trans. Power. Electron.*, 2011, **26**, (5), pp. 1377–1384
- 10 Sharma, S., Singh, B.: 'Control of permanent magnet synchronous generator-based stand-alone wind energy conversion system', *IET Power Electron.*, 2012, **5**, (8), pp. 1519–1526
- 11 Morimoto, S., Nakayama, H., Sanada, M., Takeda, Y.: 'Sensorless output maximization control for variable-speed wind generation system using IPMSG', *IEEE Trans. Ind. Appl.*, 2005, **41**, (1), pp. 60–67
- 12 Hua, G., Yang, E.X., Jiang, Y., Lee, F.C.: 'Novel zero-current-transition PWM converters', *IEEE Trans. Power. Electron.*, 1994, **9**, (6), pp. 601–606
- 13 Wang, C.M., Su, C.H., Tao, C.W.: 'Zero-current-transition PWM DC-DC converters using new zero-current-switching PWM switch cell', *IEE Proc., Electr. Power Appl.*, 2006, **153**, (4), pp. 503–512
- 14 Tseng, K.S., Liang, T.J.: 'Novel high-efficiency step-up converter', *IEE Proc., Electr. Power Appl.*, 2004, **151**, (2), pp. 182–190
- 15 Wai, R.J., Duan, R.Y.: 'High step-up converter with coupled-inductor', *IEEE Trans. Power Electron.*, 2005, **6**, (5), pp. 1025–1035
- 16 Lubosny, Z.: 'Wind turbine operation in electric power systems: advance modeling' (Berlin Heidelberg, Springer-Verlag, 2003)
- 17 Vas, P.: 'Vector control of AC machines' (Oxford University Press, New York, 1990)